
Towards One Model for Classical Dimensionality Reduction: A Probabilistic Perspective on UMAP and t-SNE

Aditya Ravuri

Neil D. Lawrence

University of Cambridge

Abstract

This paper shows that dimensionality reduction methods such as UMAP and t-SNE, can be approximately recast as MAP inference methods corresponding to a model introduced in Ravuri et al. (2023), that describes the graph Laplacian (an estimate for the precision/inverse covariance) matrix using a Wishart distribution, with a mean given by a non-linear covariance function evaluated on the latents. This interpretation offers deeper theoretical and semantic insights into such algorithms, by showing that variances corresponding to these covariances are low (and misspecified), and forging a connection to Gaussian process latent variable models by showing that well-known kernels can be used to describe covariances implied by graph Laplacians. We also introduce tools with which similar dimensionality reduction methods can be studied, and pose two areas of research arising from these interpretations.

1 Introduction

In various domains, such as single-cell biology, with complex, high-dimensional data, dimensionality reduction (DR) algorithms are essential tools for uncovering the underlying structure of data. These algorithms, which include very widely-used techniques like t-SNE (van der Maaten and Hinton, 2008) and UMAP (McInnes et al., 2020), are especially valuable for visualizing data manifolds, enabling downstream processing, and the discovery of insightful clusters and trajectories. A deeper comprehension of these algorithms and their theoretical underpinnings is crucial

for advancing their applicability, particularly when prior information is available and improving their interpretability. Our work builds on (and aims to unify fully) the ProbDR framework, which interprets classical DR methods through a probabilistic lens to enable the communication of assumptions, integration of prior knowledge and model extension for new applications.

Ravuri et al. (2023) introduced ProbDR as a framework with two main interpretations:

1. UMAP and t-SNE corresponding to inference over a nearest neighbour adjacency matrix with variational constraints, and,
2. other classical eigendecomposition-based DR algorithms as inference algorithms of a Wishart generative model on the covariance/precision matrix.

In this work, we further simplify the framework, moving away from the variational interpretation and propose that **all algorithms** with ProbDR interpretations (and hence most classical DR methods) can be written as MAP inference algorithms given the model,

$$\mathbf{S}|\mathbf{X} \sim \mathcal{W}^{\{-1\}}(K(\mathbf{X}), \nu), \quad (1)$$

where $\mathbf{S} \in S_n^+$ is an estimate of a covariance matrix generated using the high-dimensional data $\mathbf{Y} \in \mathbb{R}^{n,d}$, $\mathbf{X} \in \mathbb{R}^{n,q}$ corresponds to the set of low (q -)dimensional latent variables, and K is a positive definite matrix constructed using a covariance function/kernel acting on the embeddings.

We aim to interpret DR algorithms such as t-SNE and UMAP as MAP inference methods instead of variational methods as studied in Ravuri et al. (2023); Van Assel et al. (2022) in an effort to show what modelling assumptions give rise to the behaviour of such algorithms. Moreover, we aim to state an interpretation using a distribution such as the Wishart (as opposed to a multivariate Bernoulli) to be able to make easy comparisons between the various algorithms that exist.

Toward that end, we approximate the workings of algorithms such as UMAP and t-SNE in the **large- n**

limit and show that the bound optimised is a lower bound on the likelihood implied by the model in eq. (1). This unifies t-SNE and UMAP-like algorithms with the other algorithms and shows that UMAP and t-SNE-like algorithms differ from other DR methods by utilising a non-linear covariance function and using a very small scale parameter associated with the covariance, that depends on the hyperparameters such as number of neighbours. Additionally, along with Ravuri et al. (2023), we hope that the tools introduced in this paper will provide researchers with more machinery to extend this work and understand the behaviour of other latent variable models.

2 Background

The ProbDR framework showed that many classical DR algorithms can be expressed as inference algorithms corresponding to a probabilistic model. Algorithms that set the embedding of a high-dimensional dataset $\mathbf{Y} \in \mathbb{R}^{n,d}$ in terms of the eigenvectors of a positive-semi-definite matrix were shown in Ravuri et al. (2023) to correspond to a two-step inference process, where,

1. one first estimates a covariance matrix $\mathbf{S}(\mathbf{Y})$ or a precision matrix $\mathbf{\Gamma}(\mathbf{Y})$ (which a graph Laplacian \mathbf{L} can be an estimate of) using the data \mathbf{Y} ,
2. then estimates the embedding via maximum a-posteriori given one of the two following models,

$$\begin{aligned} \mathbf{S}|\mathbf{X} &\sim \mathcal{W}(\mathbf{X}\mathbf{X}^T + \sigma^2\mathbf{I}_n, d) \text{ or,} \\ \mathbf{\Gamma}|\mathbf{X} &\sim \mathcal{W}((\mathbf{X}\mathbf{X}^T + \beta\mathbf{I}_n)^{-1}, d). \end{aligned}$$

PCoA, for example, is recovered using the first of these formulations with $\mathbf{S} \equiv \mathbf{Y}\mathbf{Y}^T$. Setting $K(\mathbf{X}) = \mathbf{X}\mathbf{X}^T + \sigma^2\mathbf{I}$ (i.e. linear plus noise kernels) in eq. (1) recovers these results. Note that we assume an improper prior on the latents, $p(\mathbf{X}) \propto 1$, throughout this work.

In the case of UMAP and t-SNE, ProbDR did not specify a generative model for either the data or the covariance but only a generative model for the adjacency matrices that describe the nearest neighbour graph.

Specifically, ProbDR showed that the generative models corresponding to UMAP and t-SNE can be seen as models for adjacency matrices \mathbf{A}' ,

$$p(\mathbf{A}'|\mathbf{X}) = \begin{cases} \text{Categ}(\text{vec}(\mathbf{A}')|w_{ij}^t(\mathbf{X})) & \text{t-SNE} \\ \prod_{i>j}^n \text{Bern}(\mathbf{A}'_{ij}|w_{ij}^U(\mathbf{X}_i, \mathbf{X}_j)) & \text{UMAP} \end{cases} \quad (2)$$

where,

$$\begin{aligned} w_{ij}^t &= \frac{(1 + \|\mathbf{X}_i - \mathbf{X}_j\|^2)^{-1}}{\sum_{k \neq l} (1 + \|\mathbf{X}_k - \mathbf{X}_l\|^2)^{-1}}, \text{ and} \\ w_{ij}^U &= \frac{1}{1 + \|\mathbf{X}_i - \mathbf{X}_j\|^2}. \end{aligned}$$

UMAP and t-SNE, in Ravuri et al. (2023), were interpreted in a variational way, i.e. as KL-minimising algorithms, given a set of variational probabilities that depend on the empirical nearest-neighbour adjacency matrix $\mathbf{A}'(\mathbf{Y})$ computed using the data $\mathbf{Y} \in \mathbb{R}^{n,d}$ and distances between these points. Note that if the variational probabilities are zero or one, the interpretation becomes equivalent to MAP estimation (due to the Ravuri et al. (2023), Appendix B.7, Lemma 13, also presented in Damrich et al. (2022)).

Damrich et al. (2022) propose a simplification of exactly this kind: to replace the variational distributions by the binary adjacency matrix, hence, turning the algorithms into MAP-like algorithms. This simplification is reasonable due to the findings of Damrich and Hamprecht (2021), where it was found that the relatively complex calculation of the variational probabilities in t-SNE and UMAP can be replaced with simply the adjacency matrices without loss of performance. Our initial experiments also closely aligned with these findings.

Crucially, however, Becht et al. (2019); Damrich et al. (2022) note that the optimisation process is equally as important. As part of an extensive study on the nature of the t-SNE and UMAP loss functions, Damrich et al. (2022) then show how the stochastic optimisation of t-SNE and UMAP can be interpreted to be contrastive estimation with the energy function (negative loss),

$$\begin{aligned} \mathcal{E}(\mathbf{X}) &\propto \sum_{ij} \mathbf{A}_{ij} \log \left(\frac{1}{d_{ij}(\mathbf{X})^2 + 1} \right) + \\ &\frac{n-n_{\#}}{n} \sum_{ij} (1 - \mathbf{A}_{ij}) \log \left(1 - \frac{1}{d_{ij}(\mathbf{X})^2 + 1} \right), \quad (3) \end{aligned}$$

where \mathbf{A}_{ij} represents whether data points \mathbf{Y}_i and \mathbf{Y}_j are neighbours. We will refer to this as the **CNE bound**. Note that we've made some substitutions in the original formation that appears in Damrich et al. (2022), for example, we set their parameter $\tilde{q}_{ij} = 1/d_{ij}^2$, which corresponds to the UMAP setting. The hyperparameter n_- sets the number of contrastive negatives (set to be five) that affects the strength of repulsion, and $n_{\#}$ corresponds to the average number of neighbours set for a point (ten in this work). This bound is important, as we found that a naive optimisation of the Bernoulli likelihood in eq. (2) leads to a poor embedding.

For this work, we will work with this loss function and interpret it as a likelihood, but over the latents \mathbf{X} . We were particularly inspired to look toward contrastive methods by Nakamura et al. (2023), who showed that contrastive learning methods could be seen as variational algorithms (hence suggesting a link between t-SNE/UMAP and contrastive learning) and by Gutmann and Hyvärinen (2010), which shows that contrastive losses are estimators of negative log-likelihoods. Damrich et al. (2022) offer us a constrastive bound for t-SNE and UMAP, greatly simplify the optimisation process and offer a clear bound to work with, i.e. eq. (3).

3 Towards a distribution on \mathbf{A}_{ij}

eq. (3) is not a likelihood due to the multiplicative constant weighting the contribution of points that are not adjacent. The second term, \mathcal{T}_b can be expressed as follows,

$$\mathcal{T}_b = \sum_{ij} (1 - \mathbf{A}_{ij}) \log \left(\left[1 - \frac{1}{d_{ij}(\mathbf{X})^2 + 1} \right]^{\tilde{n}} \right).$$

The implied probability of adjacency $\tilde{\mathbf{p}}_{ij}$, assuming that this is the second term of a Bernoulli likelihood is,

$$\begin{aligned} \tilde{\mathbf{p}}_{ij} &= 1 - \left[1 - \frac{1}{d_{ij}(\mathbf{X})^2 + 1} \right]^{\tilde{n}} \\ &= 1 - \exp \left[\tilde{n} \log \left(1 - \frac{1}{d_{ij}(\mathbf{X})^2 + 1} \right) \right] \\ &= 1 - \exp \left[-\tilde{n} \log \left(1 + \frac{1}{d_{ij}(\mathbf{X})^2} \right) \right] \\ &\approx 1 - 1 + \tilde{n} \log \left(1 + \frac{1}{d_{ij}(\mathbf{X})^2} \right) \quad \text{large } n. \end{aligned}$$

Now, we observe that $\log(1 + 1/x) \geq 1/(1+x)$, so,

$$\begin{aligned} \mathcal{T}_b &= \sum_{ij} (1 - \mathbf{A}_{ij}) \log(1 - \tilde{\mathbf{p}}_{ij}) \\ &\leq \sum_{ij} (1 - \mathbf{A}_{ij}) \log \left(1 - \tilde{n} \frac{1}{1 + d_{ij}(\mathbf{X})^2} \right). \end{aligned}$$

Therefore,

$$\begin{aligned} \mathcal{E}(\mathbf{X}) &\leq \sum_{ij} \mathbf{A}_{ij} \log \left(\tilde{n} \frac{1}{1 + d_{ij}(\mathbf{X})^2} \right) + \\ &\quad \sum_{ij} (1 - \mathbf{A}_{ij}) \log \left(1 - \tilde{n} \frac{1}{1 + d_{ij}(\mathbf{X})^2} \right) + c. \end{aligned}$$

We conclude that the CNE bound lower bounds the Bernoulli likelihood implied by the model,

$$\mathbf{A}_{ij|\mathbf{X}} \sim \text{Bernoulli} \left(\tilde{n} \frac{1}{1 + d_{ij}(\mathbf{X})^2} \right). \quad (4)$$

The distribution in eq. (4) in itself is a good interpretation to have a probabilistic model that approximates UMAP and t-SNE, but we will go slightly further and outline an argument that makes this interpretation comparable to the interpretations in ProbDR. The utility of the Bernoulli result above is that it serves as a stepping-stone for our Wishart interpretation.

4 Towards a Wishart distribution on \mathbf{L}

In this section, we try to derive a distribution on the graph Laplacian, $\mathbf{L} = \mathbf{D} - \mathbf{A}$, where \mathbf{D} is a diagonal matrix containing the degrees $\mathbf{D}_{ii} = \sum_k \mathbf{A}_{ik}$, such that it leads to a likelihood for \mathbf{X} that approximates the CNE objective in eq. (3).

Consider the likelihood for \mathbf{X} implied by eq. (4),

$$\begin{aligned} \log p(\mathbf{X}|\mathbf{A}) &= \sum_{ij} \mathbf{A}_{ij} \log \left(\tilde{n} \frac{1}{1 + d_{ij}(\mathbf{X})^2} \right) + \\ &\quad \sum_{ij} (1 - \mathbf{A}_{ij}) \log \left(1 - \tilde{n} \frac{1}{1 + d_{ij}(\mathbf{X})^2} \right) \\ &\approx \sum_{ij} \mathbf{A}_{ij} \log \left(\tilde{n} \frac{1}{1 + d_{ij}(\mathbf{X})^2} \right) + \\ &\quad \sum_{ij} \log \left(1 - \tilde{n} \frac{1}{1 + d_{ij}(\mathbf{X})^2} \right) \quad \text{large } n \\ &\approx \text{tr}(\mathbf{A}\mathbf{P}') - \sum_{ij} \tilde{n} \frac{1}{1 + d_{ij}(\mathbf{X})^2} \quad \text{small } \tilde{n} \\ &= -\text{tr}(\mathbf{L}\mathbf{H}\mathbf{P}'\mathbf{H}) - \sum_{ij} \tilde{n} \frac{1}{1 + d_{ij}(\mathbf{X})^2} + c, \quad \text{contd. } \mathbf{L} \end{aligned}$$

where $\mathbf{P}_{ij} = \tilde{n}(1 + d_{ij}^2)^{-1}$, $\mathbf{P}'_{ij} = \log \mathbf{P}_{ij}$ and $\mathbf{H} = \mathbf{I} - \mathbf{1}\mathbf{1}^T/n$ is a centering matrix. Note that $\text{tr}(\mathbf{H}\mathbf{M}\mathbf{H}) = n - \sum_{ij} \mathbf{M}_{ij}/n$. Therefore,

$$\begin{aligned} \log p(\mathbf{X}|\mathbf{L}) &= -\text{tr}(\mathbf{L}\mathbf{H}\mathbf{P}'\mathbf{H}) + n\text{tr}(\mathbf{H}\mathbf{P}\mathbf{H}) + k \\ &\approx -\text{tr}(\mathbf{L}\mathbf{H}\mathbf{P}'\mathbf{H}) + n\log|\mathbf{I} + \mathbf{H}\mathbf{P}\mathbf{H}|. \quad \text{small } \tilde{n} \end{aligned}$$

Define $\tilde{\mathbf{L}} = \mathbf{L}/\tilde{n} = n\mathbf{L}/(n_{\#}n_-)$, noting that $\mathbf{L}/n_{\#}n_-$ is roughly a degree-normalized Laplacian. Further, we approximate $\log \mathbf{P}_{ij}$ within the vicinity of $2\tilde{n}$ by matching the gradient and function value as,

$$\log \mathbf{P}_{ij} \approx \frac{\mathbf{P}_{ij}}{\tilde{n}} - \frac{\tilde{n}}{\mathbf{P}_{ij}} + c.$$

Note that \tilde{n} is the maximal value of \mathbf{P}_{ij} . So,

$$\begin{aligned} \log p(\mathbf{X}|\mathbf{L}) &= -\text{tr}(\tilde{\mathbf{L}}\mathbf{H}\tilde{n}\mathbf{P}'\mathbf{H}) + n\log|\mathbf{I} + \mathbf{H}\mathbf{P}\mathbf{H}| + c \\ &\approx -\text{tr}(\tilde{\mathbf{L}}\mathbf{H}(\mathbf{P} - \tilde{n}^2[1/\mathbf{P}]_{ij})\mathbf{H}) + n\log|\mathbf{I} + \mathbf{H}\mathbf{P}\mathbf{H}| + c \\ &= -\text{tr}(\tilde{\mathbf{L}}(\mathbf{I} + \mathbf{H}\mathbf{P}\mathbf{H} + 2\tilde{n}\mathbf{X}\mathbf{X}^T)) + n\log|\mathbf{I} + \mathbf{H}\mathbf{P}\mathbf{H}| + k \\ &\leq \log \mathcal{W}(\tilde{\mathbf{L}}|(\mathbf{I} + \mathbf{H}\mathbf{P}\mathbf{H} + 2\tilde{n}\mathbf{X}\mathbf{X}^T)^{-1}, n). \end{aligned}$$

Therefore, the model,

$$\frac{1}{n-n_{\#}} n\mathbf{L}|\mathbf{X} \sim \mathcal{W}((\mathbf{I} + \mathbf{H}\mathbf{P}\mathbf{H} + 2\hat{n}\mathbf{X}\mathbf{X}^T)^{-1}, n) \quad (5)$$

approximates the model in eq. (4).

\mathbf{P}' is conditionally positive definite (CPD) as \mathbf{P}_{ij} defines the student-t kernel, which enforces PDness and an elementwise log of a PD matrix with all positive elements will at least be CPD (Bhatia (2007)). Double centering such matrices makes them PSD.

Interestingly, the model of eq. (5) is a non-linear extension of ProbDR’s Laplacian Eigenmaps with a non-linear kernel.

An important note here is that **the model remains misspecified** (as the variance implied by the non-noise terms of the covariance parameter of the Wishart is non-intuitive, being much lower than unity).

5 Discussion

In this paper, we’ve presented an interpretation for UMAP and t-SNE-like algorithms and proposed a comparable distributional assumption to ProbDR’s. Our model for UMAP and t-SNE-like algorithms uses a covariance based on a double-centred non-linear kernel however, as opposed to the linear kernel used as part of ProbDR’s Wishart-based algorithms.

fig. 1 shows a comparison between embeddings found with our interpretations compared with those presented in Damrich et al. (2022) within different datasets (found within the openTSNE repositories (Poličar et al., 2024)). We resample each dataset such that it has exactly 10 groups, with up to 25k points in total. The optimisation was done using a small-range GPU capable of inverting matrices of 25k rows/columns, using pytorch’s Adam optimiser, with an initial learning rate set to 1.0, with each experiment being run for 50 epochs.

We see that the embeddings recovered using our methods are qualitatively quite similar to that of CNE, with one important observation, which is that our embeddings are more t-SNE-like and CNE’s are more UMAP-like (note that CNE was run using the UMAP settings). This is likely due to our interpretations implicitly varying the “Z” parameter set in Damrich et al. (2022) which controls how t-SNE-like or UMAP-like the resultant embeddings are. Interestingly, the Bernoulli interpretation forces the embeddings to be more UMAP-like than t-SNE-like, as shown in fig. 2.



Figure 2: MNIST embeddings generated using the Bernoulli interpretation of eq. (4), which are qualitatively more UMAP-like, as opposed to the embeddings in fig. 1 generated using the Wishart interpretation.

The Wishart model of eq. (5) is quite elegant, as it implies that the data covariance is modelled by a covariance function, connecting Gaussian process latent variable models Lawrence (2005) (that use kernels not unlike the Student-t kernel to model the covariance) to ProbDR models that describe the graph Laplacian (which describes a precision matrix). Moreover, as in the case of ProbDR, we find that these models appear misspecified, as the variance corresponding to the Student-t kernel (equivalently, the probabilities of adjacency) is set to be very low. We show exactly what this small multiplicative factor is, in terms of the number of nearest neighbours set, the number of contrastive negatives, and the number of data points. The semantic, probabilistic, and modelling implications behind such misspecified assumptions remain an area that needs to be studied.

In addition to these insights, we show non-traditional ways in which covariances can be constructed as part of Gaussian process models and/or dimensionality reduction methods, which revolve around double-centering CPD matrices (which can be based on distance matrices).

For example, take $-\mathbf{D}' = \log \frac{1}{1 + \|\mathbf{X}_i - \mathbf{X}_j\|^2}$, where \mathbf{D} represents a distance matrix. The inner term is a kernel, hence is PSD. The log function (like the square root, in this context) preserves CPSD-ness (Bhatia, 2007). Therefore, $-\mathbf{H}\mathbf{D}\mathbf{H}$ is PSD. It’s also interesting to observe, due to the results of Khare (2019); Schoenberg (1935), that there exists an isometric Euclidean embedding for such a distance matrix (and vice versa).

Other empirical arguments can also be made to show that, assuming a model such as: $\mathbf{X} \rightarrow \mathbf{Y} \rightarrow \mathbf{A}$, where

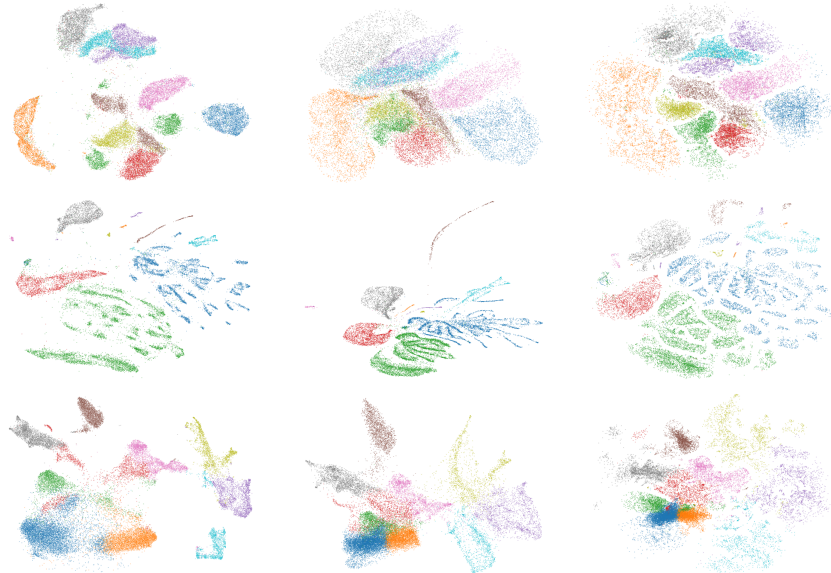


Figure 1: Comparison between using the CNE bound (eq. (3), **left**), our Wishart likelihood (eq. (5), **center**) and our Wishart model with an alternative covariance parameter, $\mathbf{C} = \mathbf{I} + \mathbf{H}\mathbf{P}^o\mathbf{H}$, with $\mathbf{P}_{ij}^o = \sqrt{\mathbf{P}_{ij}/(\sum_k \mathbf{P}_{ik} \sum_{k'} \mathbf{P}_{jk'})}$ (**right**) for dimensionality reduction. The covariance used on the right was inspired by moment-matching arguments and is similar to our proposed model, as double centering \mathbf{P}' leads to the element-wise log of the normed matrix in \mathbf{P}^o plus a constant that disappears in the trace operation. **Top row**: MNIST digits, **middle row**: mouse retinal transcriptomic data from Macosko et al. (2015) and **bottom row**: larger scale transcriptomic data from Zheng et al. (2017).

$\mathbf{Y}|\mathbf{X} \sim \mathcal{N}$, the adjacency probabilities of eq. (4) cannot be found using simply a linear kernel, and **can** be found using a non-linear kernel such as a Student-t kernel, as we’ve used here. For this, one can write out the approximate distribution on distances (assuming a Gaussian process prior on \mathbf{Y} , $\mathbb{E}(d_{ij}^2(\mathbf{Y})) = d^*(k_{ii} + k_{jj} - 2k_{ij})$ and $\text{Cov}(d_{ij}^2, d_{mn}^2) = 2d^*(k_{im} + k_{jn} - k_{in} - k_{jm})^2$) and study the probability with which such distances attain extreme values, as a function of latent distance.

Lastly, the fact that our implied covariance is non-stationary can be justified by the fact that the adjacency probabilities go to zero as a function of distance (which is atypical in contrast to GPLVM literature, where the use of stationary kernels is a norm).

6 Conclusion

In conclusion, this study presents a novel theoretical framework that reinterprets UMAP and t-SNE-like algorithms as maximum a posteriori (MAP) inference algorithms within a model for a graph Laplacian described by a Wishart distribution. This result bridges the gap between popular dimensionality reduction methods with Gaussian process latent variable models, enhancing our understanding of their mechanisms. The insights gained show the importance of specific modelling assumptions in optimizing these al-

gorithms’ effectiveness and interpretability, setting a foundation for further research on model specifications and their practical implications.

Acknowledgements

AR would like to thank Francisco Vargas for helpful discussions and a studentship from the Accelerate Programme for Scientific Discovery.

Bibliography

- Becht, E., McInnes, L., Healy, J., Dutertre, C.-A., Kwok, I. W. H., Ng, L. G., Ginhoux, F., and Newell, E. W. (2019). Dimensionality reduction for visualizing single-cell data using UMAP. *Nature Biotechnology*, 37(1):38–44.
- Bhatia, R. (2007). *Positive Definite Matrices*. Princeton University Press.
- Damrich, S., Böhm, N., Hamprecht, F. A., and Kobak, D. (2022). From t-sne to umap with contrastive learning. In *The Eleventh International Conference on Learning Representations*.
- Damrich, S. and Hamprecht, F. A. (2021). On umap’s true loss function. In Ranzato, M., Beygelzimer, A., Dauphin, Y., Liang, P., and Vaughan, J. W., editors, *Advances in Neural Information Processing Systems*, volume 34, pages 5798–5809. Curran Associates, Inc.

- Gutmann, M. and Hyvärinen, A. (2010). Noise-contrastive estimation: A new estimation principle for unnormalized statistical models. In *Proceedings of the thirteenth international conference on artificial intelligence and statistics*, pages 297–304. JMLR Workshop and Conference Proceedings.
- Khare, A. (2019). Schoenberg: from metric geometry to matrix positivity.
- Lawrence, N. D. (2005). Probabilistic non-linear principal component analysis with Gaussian process latent variable models. *J. Mach. Learn. Res.*, 6:1783–1816.
- Macosko, E. Z., Basu, A., Satija, R., Nemesh, J., Shekhar, K., Goldman, M., Tirosh, I., Bialas, A. R., Kamitaki, N., Martersteck, E. M., Trombetta, J. J., Weitz, D. A., Sanes, J. R., Shalek, A. K., Regev, A., and McCarroll, S. A. (2015). Highly parallel genome-wide expression profiling of individual cells using nanoliter droplets. *Cell*, 161(5):1202–1214.
- McInnes, L., Healy, J., and Melville, J. (2020). UMAP: Uniform manifold approximation and projection for dimension reduction.
- Nakamura, H., Okada, M., and Taniguchi, T. (2023). Representation uncertainty in self-supervised learning as variational inference. In *Proceedings of the IEEE/CVF International Conference on Computer Vision*, pages 16484–16493.
- Poličar, P. G., Stražar, M., and Zupan, B. (2024). opentsne: A modular python library for t-sne dimensionality reduction and embedding. *Journal of Statistical Software*, 109(3):1–30.
- Ravuri, A., Vargas, F., Lalchand, V., and Lawrence, N. D. (2023). Dimensionality reduction as probabilistic inference. In *Fifth Symposium on Advances in Approximate Bayesian Inference*.
- Schoenberg, I. J. (1935). Remarks to maurice frechet’s article “sur la definition axiomatique d’une classe d’espace distances vectoriellement applicable sur l’espace de hilbert. *Annals of Mathematics*, 36(3):724–732.
- Van Assel, H., Espinasse, T., Chiquet, J., and Picard, F. (2022). A probabilistic graph coupling view of dimension reduction. *Advances in Neural Information Processing Systems*, 35:10696–10708.
- van der Maaten, L. and Hinton, G. (2008). Visualizing data using t-SNE. *Journal of Machine Learning Research*, 9(86):2579–2605.
- Zheng, G. X. Y., Terry, J. M., Belgrader, P., Ryvkin, P., Bent, Z. W., Wilson, R., Ziraldo, S. B., Wheeler, T. D., McDermott, G. P., Zhu, J., Gregory, M. T., Shuga, J., Montesclaros, L., Underwood, J. G., Masquelier, D. A., Nishimura, S. Y., Schnall-Levin, M., Wyatt, P. W., Hindson, C. M., Bharadwaj, R., Wong, A., Ness, K. D., Beppu, L. W., Deeg, H. J., McFarland, C., Loeb, K. R., Valente, W. J., Ericson, N. G., Stevens, E. A., Radich, J. P., Mikkelsen, T. S., Hindson, B. J., and Bielas, J. H. (2017). Massively parallel digital transcriptional profiling of single cells. *Nature Communications*, 8(1):14049.